Neurosci. Bull. October, 2019, 35(5):889–900
https://doi.org/10.1007/s12264-019-00395-4

www.neurosci.cn
www.springer.com/12264

ORIGINAL ARTICLE

Poly-PR in *C9ORF72*-Related Amyotrophic Lateral Sclerosis/Frontotemporal Dementia Causes Neurotoxicity by Clathrin-Dependent Endocytosis

Rui Wang[1] · Xingyun Xu[1] · Zongbing Hao[1] · Shun Zhang[1] · Dan Wu[1] · Hongyang Sun[1] · Chenchen Mu[1] · Haigang Ren[1] · Guanghui Wang[1]

Received: 10 December 2018 / Accepted: 22 March 2019 / Published online: 30 May 2019

Abstract GGGGCC repeat expansions in the *C9ORF72* gene are the most common cause of amyotrophic lateral sclerosis and frontotemporal dementia (c9ALS/FTD). It has been reported that hexanucleotide repeat expansions in *C9ORF72* produce five dipeptide repeat (DPR) proteins by an unconventional repeat-associated non-ATG (RAN) translation. Within the five DPR proteins, poly-PR and poly-GR that contain arginine are more toxic than the other DPRs (poly-GA, poly-GP, and poly-PA). Here, we demonstrated that poly-PR peptides transferred into cells by endocytosis in a clathrin-dependent manner, leading to endoplasmic reticulum stress and cell death. In SH-SY5Y cells and primary cortical neurons, poly-PR activated JUN amino-terminal kinase (JNK) and increased the levels of p53 and Bax. The uptake of poly-PR peptides by cells was significantly inhibited by knockdown of clathrin or by chlorpromazine, an inhibitor that blocks clathrin-mediated endocytosis. Inhibition of clathrin-dependent endocytosis by chlorpromazine significantly blocked the transfer of poly-PR peptides into cells, and attenuated poly-PR-induced JNK activation and cell death. Our data revealed that the uptake of poly-PR undergoes clathrin-dependent endocytosis and blockade of this process prevents the toxic effects of synthetic poly-PR peptides.

Keywords Amyotrophic lateral sclerosis · *C9ORF72* · Poly-PR · Clathrin · ER stress

Introduction

Amyotrophic lateral sclerosis (ALS) is a devastating neurodegenerative disorder characterized by progressive loss of motor neurons in the brain and spinal cord [1, 2]. The expansions of hexanucleotide (GGGGCC) repeats in the gene *chromosome 9 open reading frame 72* (*C9ORF72*) is the most common cause of ALS and frontotemporal dementia (FTD) [3, 4]. The expanded hexanucleotide repeats can be transcribed to sense and antisense RNA foci and further translated into dipeptide repeat (DPR) proteins through an unconventional form of non-ATG (RAN) translation [5–8]. Previous studies in flies and cultured cells have suggested that the production of DPRs is one of the important drivers of neurodegeneration in *C9ORF72*-related ALS/FTD [9–11]. The arginine-rich DPRs, glycine-arginine (GR) and proline-arginine (PR), are highly toxic to cultured cells through nucleolar stress, oxidative stress, compromising nucleocytoplasmic transport, and dysregulating the dynamics of membrane-less organelles [12–19].

Previous studies have reported that the cell-to-cell spread of DPRs *via* exosome-dependent and -independent pathways may be relevant to the disease [20]. In addition, synthetic poly-PR and poly-GR peptides added to the culture medium can be taken up by cells, inducing cell toxicity in a dose-dependent manner by disrupting RNA biogenesis or inhibiting translation [10, 21, 22].

Rui Wang, Xingyun Xu and Zongbing Hao have contributed equally to this work.

Electronic supplementary material The online version of this article (https://doi.org/10.1007/s12264-019-00395-4) contains supplementary material, which is available to authorized users.

✉ Guanghui Wang
wanggh@suda.edu.cn

[1] Laboratory of Molecular Neuropathology, Jiangsu Key Laboratory of Neuropsychiatric Diseases and Department of Pharmacology, College of Pharmaceutical Sciences, Soochow University, Suzhou 215123, China

Endoplasmic reticulum (ER) stress signaling is tightly associated with various neurodegenerative diseases, especially ALS [23–25]. In response to ER stress, a complex signaling network known as the unfolded protein response (UPR) is induced to alleviate the stress. Three factors, protein kinase RNA-like ER kinase (PERK), inositol-requiring enzyme 1 (IRE1), and activating transcription factor-6 (ATF6), differentially initiate the UPR to three distinct pathways [26–28]. The UPR signaling network is crucial for the control of protein folding, autophagy, oxidant regulation, and amino-acid metabolism upon ER stress [23]. However, sustained or chronic ER stress activates the JNK-mediated pathway or upregulates the transcription factor CHOP (C/EBP-homologous protein) that is encoded by *Ddit3* and downstream of PERK, which induces cell death [29, 30]. In the superoxide dismutase (SOD1)-ALS model, the activation of PERK and IRE1α has been identified in spinal motor neurons, suggesting that ER stress is associated with motor neuron death. Moreover, ER stress can lead to activation of the JNK pathway, which is crucial for promoting cell death in ALS models [31–34]. Activation of ER stress has also been detected in induced pluripotent stem cell (iPSC)-derived human motor neurons and in a cellular model exposed to poly-GA (glycine-alanine) [35, 36].

Endocytosis is a cellular process involving the internalization of extracellular material, ligands and membrane proteins, and lipids [37]. The functions of endocytosis are not only the absorption of extracellular materials, but also the regulation of various processes initiated at the cell surface. Endocytosis processes can be subdivided into four categories: macropinocytosis, clathrin-mediated endocytosis, caveola-dependent endocytosis, and clathrin- and caveola-independent endocytosis. Although these pathways are different, specific endocytic components can participate in other pathways [38, 39]. Neurons, like other cell types, absorb extracellular materials though these pathways, but it is still unclear whether endocytic pathways are involved in poly-PR uptake. Here we showed that the clathrin-dependent endocytic pathway is involved in poly-PR-mediated neurotoxicity. Poly-PR is transferred into cells in a clathrin-dependent manner and induces cell death *via* ER stress and the JNK-mediated pathway.

Materials and Methods

Cell Culture

SH-SY5Y cells, a kind gift from Dr. Jin Xu (Institute of Neuroscience, Chinese Academy of Sciences, Shanghai, China), were cultured in Dulbecco's modified Eagle's medium (DMEM, Gibco, Grand Island, NY, USA) with 10% fetal bovine serum (FBS) including penicillin (100 μg/mL) and streptomycin (100 μg/mL). Primary mouse cortical neurons were prepared as described elsewhere [40]. In brief, the dissociated neurons were cultured in DMEM/F12 (Gibco) with 10% FBS for 6 h. Subsequently, the culture medium was changed to Neurobasal medium with 1 × B27 (B-27^{TM} Plus Neuronal Culture System, Gibco). Half of the medium was changed every 3 days. The neurons were subjected to experiments at 5 days *in vitro* (DIV5). Cells were maintained in a humidified incubator at 37°C under 5% CO_2.

Peptide Synthesis and Drug Treatment

Fluorescein isothiocyanate (FITC)-labeled PR_{20} peptides were synthesized by ChinaPeptides Co., Ltd (Shanghai, China) and dissolved in sterile water. Chlorpromazine, genistein, nystatin, and ethyl-isopropyl amiloride (EIPA) were from MedChemExpress (Monmouth Junction, NJ, USA) and dissolved with dimethylsulfoxide (DMSO). SP600125 was from Selleck (Houston, TX, USA) and dissolved with DMSO.

Flow Cytometry

To analyze the internalization of the FITC-PR_{20} peptides, SH-SY5Y cells were pretreated with or without 10 μmol/L chlorpromazine, and then treated with 5 μmol/L FITC-PR_{20} for 2 h. Then, the cells were treated with 0.05% trypsin and collected. The cells were centrifuged at 2500 rpm for 5 min and the supernatant was removed. They were then washed with PBS and centrifuged at 2000 rpm for 5 min. After the washing cycle was repeated, the cells were suspended in PBS (600 μL) and subjected to fluorescence analysis on a flow cytometer (Beckman FC-500, Miami, FL, USA).

Small Interfering RNA (siRNA)

RNA oligonucleotides were transfected into cells as described previously [41]. Briefly, the cells were incubated in a mixture of Opti-MEM, RNAiMAX (Invitrogen, Carlsbad, CA, USA) and RNA oligonucleotides for 20 min at room temperature before transfection. Twenty-four hours after transfection, the medium was replaced with fresh complete medium. The cells were collected 72 h after transfection for further analysis. Oligonucleotides that targeted human *CLTC* were from GenePharma (Shanghai, China). The sequences were as follows: si-*CLTC* #1 sense 5′-UGCUCUAUUUAUAUAGAAAUAAUTT-3′, antisense 5′-AUUAUUUCUAUAUAAAUAGAGCATT-3′; si-*CLTC* #2 sense 5′-UAGAACAUUUCACUGAUUUAUAUTT-3′, antisense 5′-AUAUAAAUCAGUGAAAUGUUCUATT-3′.

Propidium Iodide (PI) Staining Assays

SH-SY5Y cells were treated with different concentrations of PR_{20}, incubated with Hoechst 33342 (Sigma, St. Louis, MO, USA) or PI (Beyotime, Shanghai, China) for 8 min, and washed with PBS. The cells were then imaged using an inverted IX71 microscope system (Olympus, Tokyo, Japan).

Immunofluorescence

Immunofluorescence was analyzed as described previously [42]. Cells were fixed in 4% paraformaldehyde for 10 min at room temperature and permeabilized with 0.25% Triton X-100 for 10 min, blocked with 1% bovine serum albumin for 1 h, and incubated with primary antibodies overnight at 4 °C. The following primary antibodies were used: anti-cleaved caspase-3 (Cell Signaling Technology, Danvers, MA, USA, Cat# 9661), Anti-p53 (Santa Cruz Biotechnology, Santa Cruz, CA, USA, Cat# sc-126), and anti-MAP2 (Santa Cruz Biotechnology, Santa Cruz, CA, USA, Cat# sc-20172). After incubation with the primary antibodies, cells were washed three times with PBS and then incubated with rhodamine (red)-conjugated secondary antibody (Invitrogen, Carlsbad, CA, USA) for 1 h at room temperature. After incubation, the cells were stained with DAPI for 5 min and imaged using the inverted IX71 microscope system (Olympus, Tokyo, Japan).

Western Blot

Cells were lysed in 1 × SDS lysis buffer (50 mmol/L Tris-HCl (pH 7.5), 150 mmol/L NaCl, 1% Nonidet P40, and 0.5% sodium deoxycholate) supplemented with a protease inhibitor cocktail (Roche, Basel, Switzerland). About 20 μg of cell lysate was isolated by SDS-PAGE and transferred onto a PVDF membrane (Millipore, Billerica, MA, USA). Western blots were analyzed for the following primary antibodies: anti-CHOP (Abcam, Cambridge, MA, USA, Cat# ab179823), anti-p-JNK (Thr183/Tyr185), anti-JNK (Cell Signaling Technology, Danvers, MA, USA, Cat# 4668, Cat#9252), anti-p53 and anti-Bax (Santa Cruz Biotechnology, Santa Cruz, CA, USA, Cat# sc-126 and Cat# sc-493), and anti-β-actin (Sigma, St. Louis, MO, USA, A3854). The secondary antibodies, sheep anti-rabbit, or anti-mouse IgG-HRP, were from Thermo Fisher (Waltham, MA, USA). The proteins were visualized using an ECL detection kit (Thermo Fisher, Waltham, MA, USA).

Cytotoxicity Assays

Cytotoxicity was measured using lactate dehydrogenase (LDH) release assays (Promega, Madison, WI, USA, CytoTox 96 Non-Radioactive Cytotoxicity Assay). Briefly, 50 μL of CellTiter-Glo reagent was added to wells containing 50 μL of growth medium. After vigorous shaking at room temperature for 20 min, luminescence was measured to determine cell viability. Cell viability determination was performed in triplicate.

RNA Isolation and Quantitative Real-Time PCR (qRT-PCR)

Total RNA was isolated as previously described [43]. Total RNA from cells was extracted with TRIzol reagent (Invitrogen, Carlsbad, CA, USA), then the RNA was reverse-transcribed into cDNA using a TransScript First-Strand cDNA Synthesis Kit (Takara, Otsu, Shiga, Japan). Real-time PCR analysis was performed using SYBR Green Real-Time PCR Master Mix (Thermo Fisher, Waltham, MA, USA) on a 7500 Real-Time System (Thermo Fisher, Waltham, MA, USA) and the following primers: human *ATF4* sense 5'-CTCCGGGACAGATTGGATGTT-3', antisense 5'-GGCTGCTTATTAGTCTCCTGGAC-3'; human *CHOP* sense 5'-GGAAACAGAGTGGTCATTCCC-3', antisense 5'-CTGCTTGAGCCGTTCATTCTC-3'; mouse *ATF4* sense 5'-CTCTTGACCACGTTGGATGAC-3', antisense 5'-CAACTTCACTGCCTAGCTCTAAA-3'; mouse *CHOP* sense 5'-TTATCTTGAGCCTAACACGTCG-3', antisense 5'-TCAGGTGTGGTGGTGTATGAA-3'; mouse *p53* sense 5'-GCGTAAACGCTTCGAGATGTT-3', antisense 5'-TTTTTATGGCGGGAAGTAGACTG-3'; mouse *Bax* sense 5'-AGACAGGGGCCTTTTTGCTAC-3', antisense 5'-AATTCGCCGGAGACACTCG-3'; mouse *Hrk* sense 5'-GGCACGCACACAGTTCATTT-3', antisense 5'-ACACCATGGCAGAGACAGTG-3'. The mRNA expression was measured using the $\Delta\Delta Ct$ method relative to that of an endogenous control gene (*β-actin*).

Lentiviral Transduction

To generate expression vectors for EGFP-$(PR)_{28}$, the CCAAGA with 28 repeats was synthesized by Invitrogen and ligated to the EcoRI and BamHI restriction sites of a pEGFP-C1 vector (Clontech Laboratories, Mountain View, CA, USA). The transduction experiments were carried out with lentivirus Ubi-EGFP-MCS (Shanghai Genechem Co., Ltd, Shanghai, China) expressing EGFP-$(PR)_{28}$ and EGFP.

Statistical Analysis

The results were quantified using Photoshop 7.0 (Adobe, San Jose, CA, USA) and the data were analyzed using GraphPad Prism 7.00 (GraphPad Software, Version X; La Jolla, CA, USA). Significant differences were calculated using a two-tailed unpaired *t* test or one-way analysis of variance

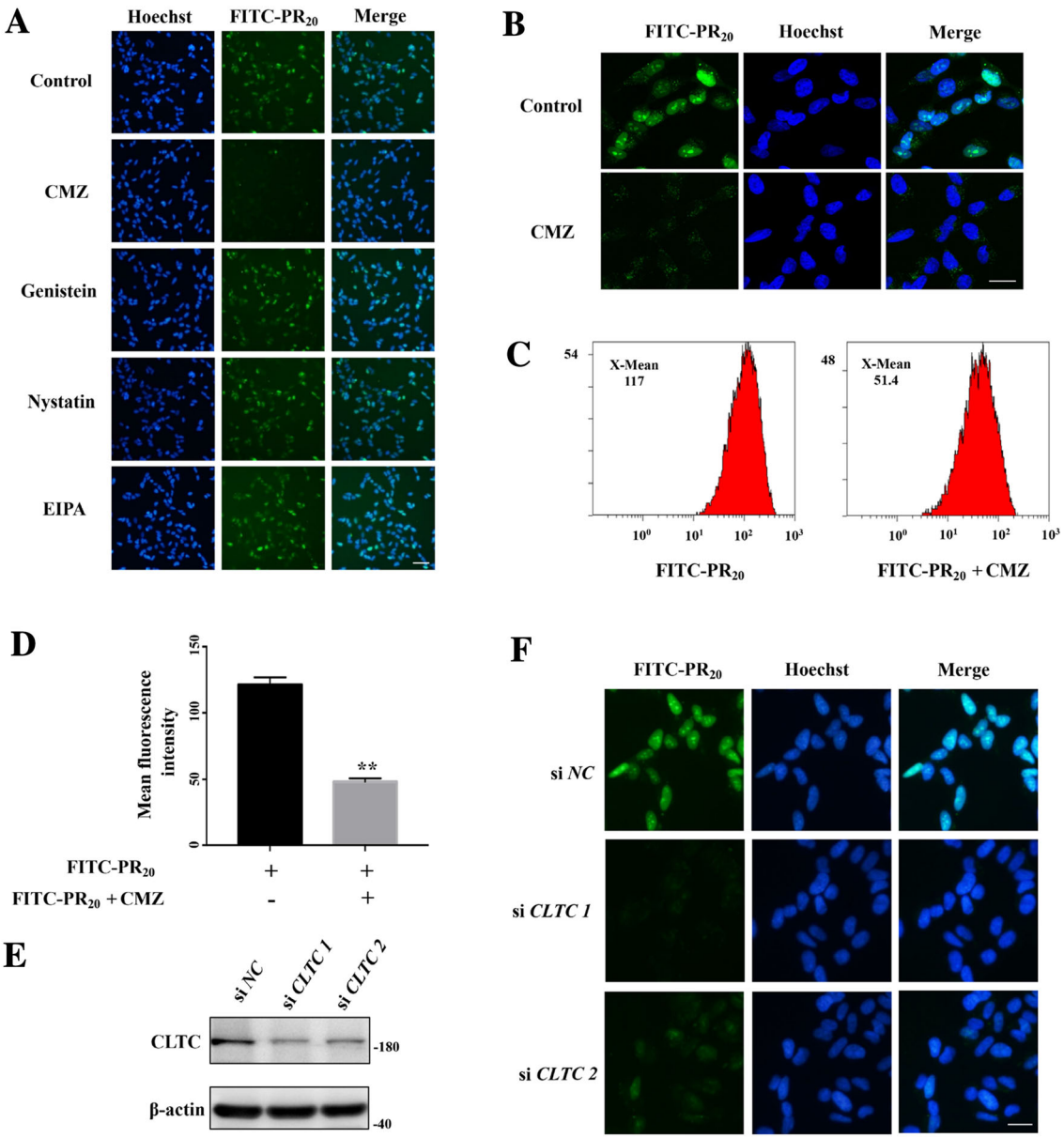

Fig. 1 Synthetic PR_{20} peptides are transferred into cells by clathrin-dependent endocytosis**. A** SH-SY5Y cells incubated with chlorpromazine (CMZ), genistein, nystatin, and EIPA (each at 10 μmol/L) for 30 min, and then further incubated with 5 μmol/L FITC-PR_{20} for 2 h (blue, Hoechst; green, FITC; scale bar, 50 μm). **B** SH-SY5Y cells incubated with CMZ (10 μmol/L) for 30 min and then further incubated with 5 μmol/L FITC-PR_{20} for 2 h (blue, Hoechst; green, FITC; scale bar, 20 μm). **C** Flow cytometric analysis of SH-SY5Y cells treated as in B (X-mean value, average fluorescence intensity of FITC). **D** Quantification of the intensity of flow cytometric fluorescence as in (C). Values are the mean ± SEM from 6 independent experiments (**$P < 0.01$, *t*-tests). **E** Western blots using clathrin heavy chain antibody in SH-SY5Y cells transiently transfected with siRNA for clathrin heavy chain for 72 h and then further incubated with 5 μmol/L FITC-PR_{20} for 2 h. **F** SH-SY5Y cells treated as in (E) (blue, Hoechst; green, FITC; scale bar, 20 μm).

(ANOVA) followed by Dunnett's multiple-comparisons test or two-way ANOVA followed by Tukey's multiple-comparisons test. The criterion of significance was set at $P < 0.05$. The values are shown as the mean ±SEM.

Results

Synthetic PR_{20} Peptides are Transferred into Cells by Clathrin-Dependent Endocytosis

To determine which endocytic pathway is involved in poly-PR uptake, we used pharmacological inhibitors of endocytosis to block specific endocytic pathways in SH-SY5Y

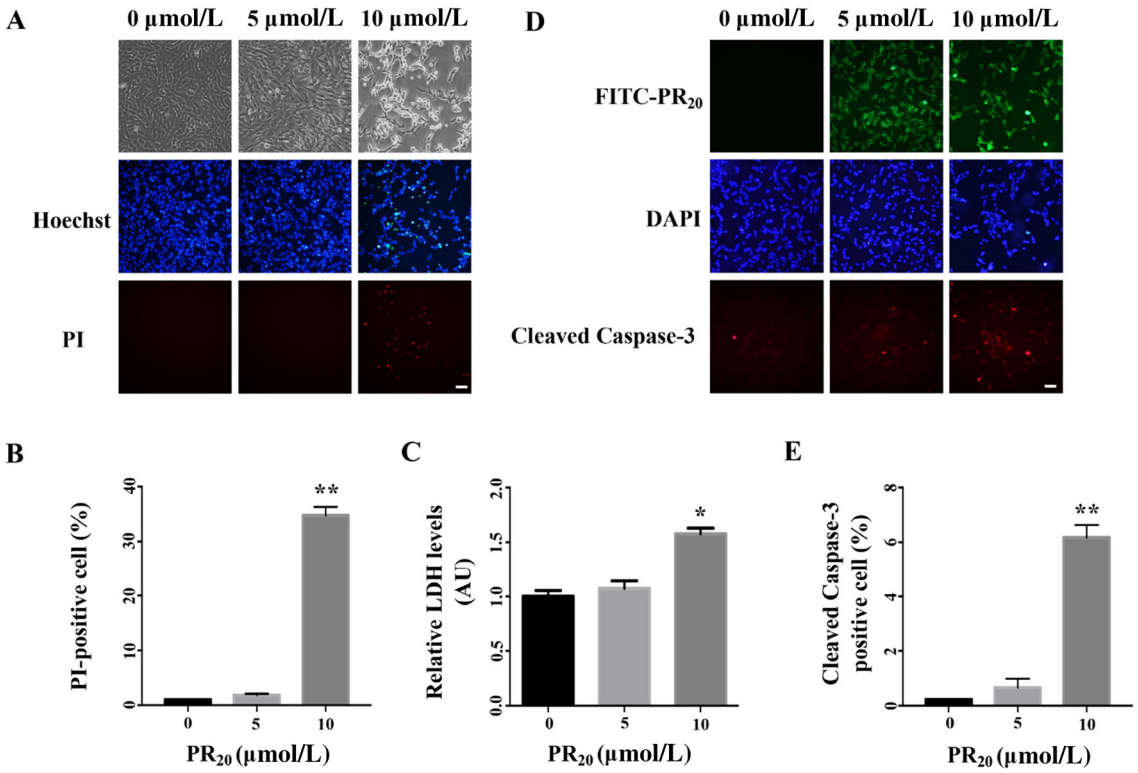

Fig. 2 Synthetic PR_{20} peptides cause cell death in SH-SY5Y cells. **A** SH-SY5Y cells treated with PR_{20} (0, 5, or 10 μmol/L) for 24 h. then stained with PI for cell death assays (blue, Hoechst; red, PI; scale bar, 100 μm). **B** Relative integrated optical density of PI-positive cells as in (A). Values are the mean ± SEM from three independent experiments (**$P < 0.01$, one-way ANOVA and Dunnett's multiple comparisons test). **C** Cytotoxicity measured using lactate dehydrogenase (LDH) release assays in SH-SY5Y cells treated with PR_{20} (0, 5, or 10 μmol/L) for 48 h. Values are the mean ± SEM from three independent experiments (*$P < 0.05$, one-way ANOVA and Dunnett's multiple comparisons test). **D** Immunofluorescence of cleaved-caspase 3 in SH-SY5Y cells treated as in A (blue, DAPI; green, FITC; red, cleaved-caspase 3; scale bar, 50 μm). **E** Quantification of the density of cleaved-caspase 3-positive cells as in (D). Values are the mean ± SEM from three independent experiments (**$P < 0.01$, one-way ANOVA and Dunnett's multiple comparisons test).

cells. Interestingly, chlorpromazine, an inhibitor of clathrin-mediated endocytosis [44, 45], blocked poly-PR transfer into cells at 10 μmol/L (Fig. 1A–C). However, genistein and nystatin, inhibitors of caveola-dependent endocytosis [46, 47], and EIPA, an inhibitor for macropinocytosis [48], did not prevent the internalization of poly-PR (Fig. 1A). In cells treated with PR_{20} for 2 h, PR_{20} was transferred into the cells and accumulated in nuclei (Fig. 1B). However, in cells treated with chlorpromazine, the abundance of PR_{20} in cells was greatly decreased compared to cells without chlorpromazine treatment (Fig. 1B–D). Moreover, PR_{20} only formed a few cytosolic puncta but did not accumulate in nuclei (Fig. 1B). To further confirm that clathrin-mediated endocytosis contributes to the transfer of poly-PR into cells, we knocked down clathrin heavy-chain (CLTC) to assess the effects of clathrin on poly-PR transfer. The uptake of PR_{20} peptides was markedly lower in SH-SY5Y cells transfected with siRNA against CLTC than with control siRNA (Fig. 1E) after treatment with synthetic PR_{20} peptides (Fig. 1F).

Synthetic PR_{20} Peptides Cause SH-SY5Y Cell Death

It has been reported that poly-PR tends to accumulate in the nucleoli and causes cell death [10]. We found that the synthetic PR_{20} was remarkably cytotoxic to SH-SY5Y cells, as evidenced by PI staining (Fig. 2A, B). In SH-SY5Y cells, synthetic PR_{20} peptides induced significant cell death at 10 μmol/L (Fig. 2B, C). Treatment of cells with synthetic PR_{20} (10 μmol/L) activated caspase-3; the percentage of cells positive for cleaved caspase-3 was ~8-fold higher than that in control cells (Fig. 2D, E).

Synthetic PR_{20} Peptides Induce Endoplasmic Reticulum Stress and JNK Activation in SH-SY5Y Cells

Since poly-PR caused significant cell death (Fig. 2), and ER stress is an important factor in cell death in neurodegenerative diseases [49], we assessed the expression of CHOP, a marker of ER stress. In SH-SY5Y cells treated with 0, 5, or 10 μmol/L synthetic PR_{20}, the mRNAs of the ER stress markers *Atf4* and *Ddit3* were significantly

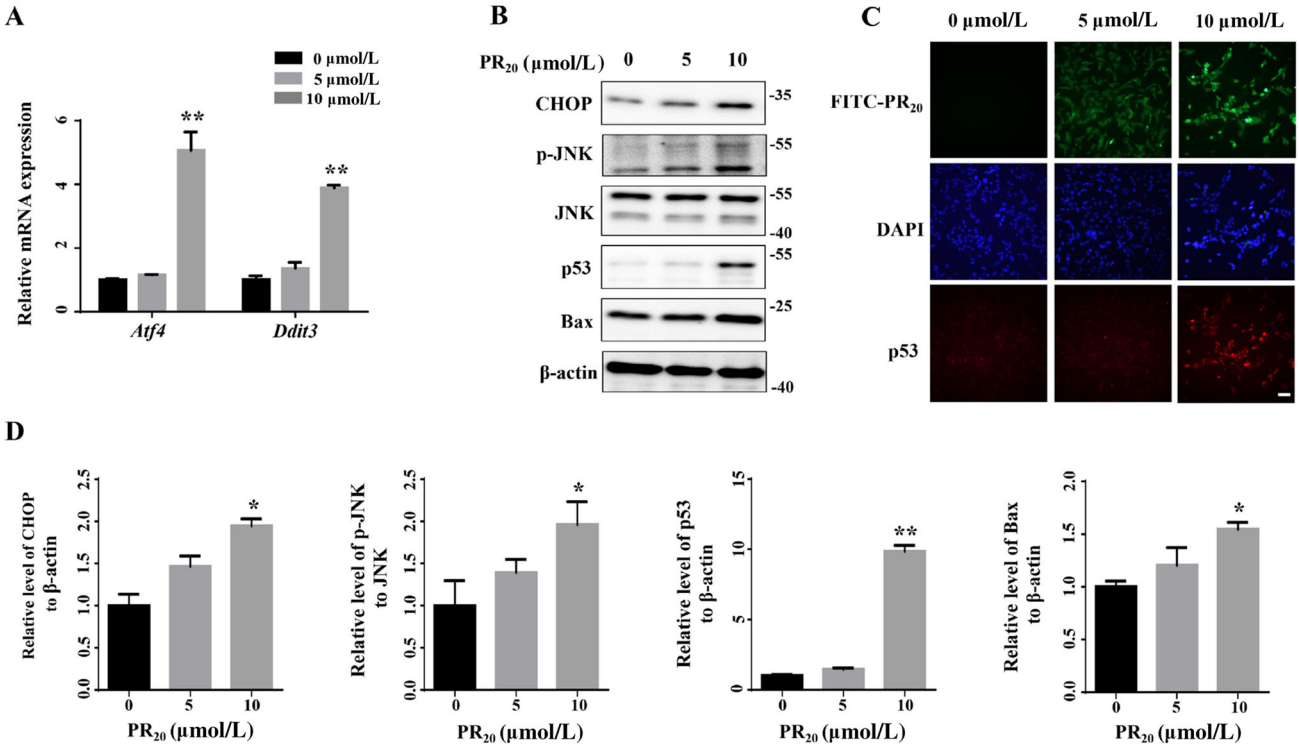

Fig. 3 Synthetic PR_{20} peptides induce endoplasmic reticulum stress and JNK activation in SH-SY5Y cells. **A** qRT-PCR analysis of SH-SY5Y cells treated with PR_{20} (0, 5, or 10 μmol/L) for 24 h. The levels of *Atf4* and *Ddit3* mRNA were quantified and normalized to *β-actin*. Values are the mean ± SEM from three independent experiments (**$P < 0.01$, one-way ANOVA and Dunnett's multiple comparisons test). **B** Western blots of CHOP, p-JNK, p53, and Bax protein levels in SH-SY5Y cells treated as in (A). **C** Immunofluorescent staining of p53 in SH-SY5Y cells treated as in (A) (blue, DAPI; green, FITC; red, p53; scale bar, 50 μm). **D** Quantitative analysis of the relative density of CHOP, p53, and Bax normalized to the loading control (β-actin) and quantitative analysis of the relative density of p-JNK normalized to the loading control (JNK). Values are the mean ± SEM from three independent experiments (*$P < 0.05$, **$P < 0.01$, one-way ANOVA and Dunnett's multiple comparisons test).

upregulated 10 μmol/L synthetic PR_{20} (Fig. 3A). Consistently, the CHOP protein level was increased in cells treated with 10 μmol/L synthetic PR_{20} (Fig. 3B, D). It has been reported that ER stress induces cell death through activation of the JNK-mediated pathway [29]. We therefore examined the activation of JNK by evaluating its phosphorylation. In SH-SY5Y cells treated with PR_{20} at 10 μmol/L, the phosphorylation of JNK was significantly increased (Fig. 3B, D). Moreover, the protein levels of p53 and the pro-apoptotic factor Bax were increased in SH-SY5Y cells that with 10 μmol/L PR_{20} (Fig. 3B, D). Immunofluorescent staining further showed an increase of p53 levels after treatment with 10 μmol/L PR_{20} (Fig. 3C).

Poly-PR Induces ER Stress and JNK Activation in Primary Cortical Neurons of Mouse

As poly-PR is toxic to cultured cell lines, we evaluated whether poly-PR is harmful to mouse primary cortical neurons. The primary cortical neurons were treated with different concentrations of synthetic PR_{20}, and the cell death was evaluated using LDH release assays. Similar to the data from cultured cell lines, synthetic PR_{20} peptides also induced neuronal death, but at a concentration as low as 0.5 μmol/L (Fig. 4A), showing that primary cultured neurons are sensitive to poly-PR. In primary neurons treated with 0.5 μmol/L PR_{20}, the expression of CHOP and Bax, and the phosphorylation of JNK were increased (Fig. 4B and 4C). To evaluate the effects of ploy-PR in a more disease-relevant context, we generated lentivirus vectors expressing PR with 28 repeats. The expression of *Chop*, *Atf4*, *p53*, *Bax*, and *Hrk* was significantly upregulated in primary neurons that expressed GFP-PR_{28} but not in those that expressed GFP alone (Fig. 4D). Meanwhile, the phosphorylation of JNK and the expression of Bax were upregulated in neurons expressing the poly-PR lentivirus (Fig. 4E, F).

JNK Inhibitor SP600125 Suppresses the Cell Death Caused by PR_{20}

To further determine whether the activation of the JNK pathway plays a crucial role in the cell death induced by PR_{20}, we used the JNK inhibitor SP600125 to block JNK

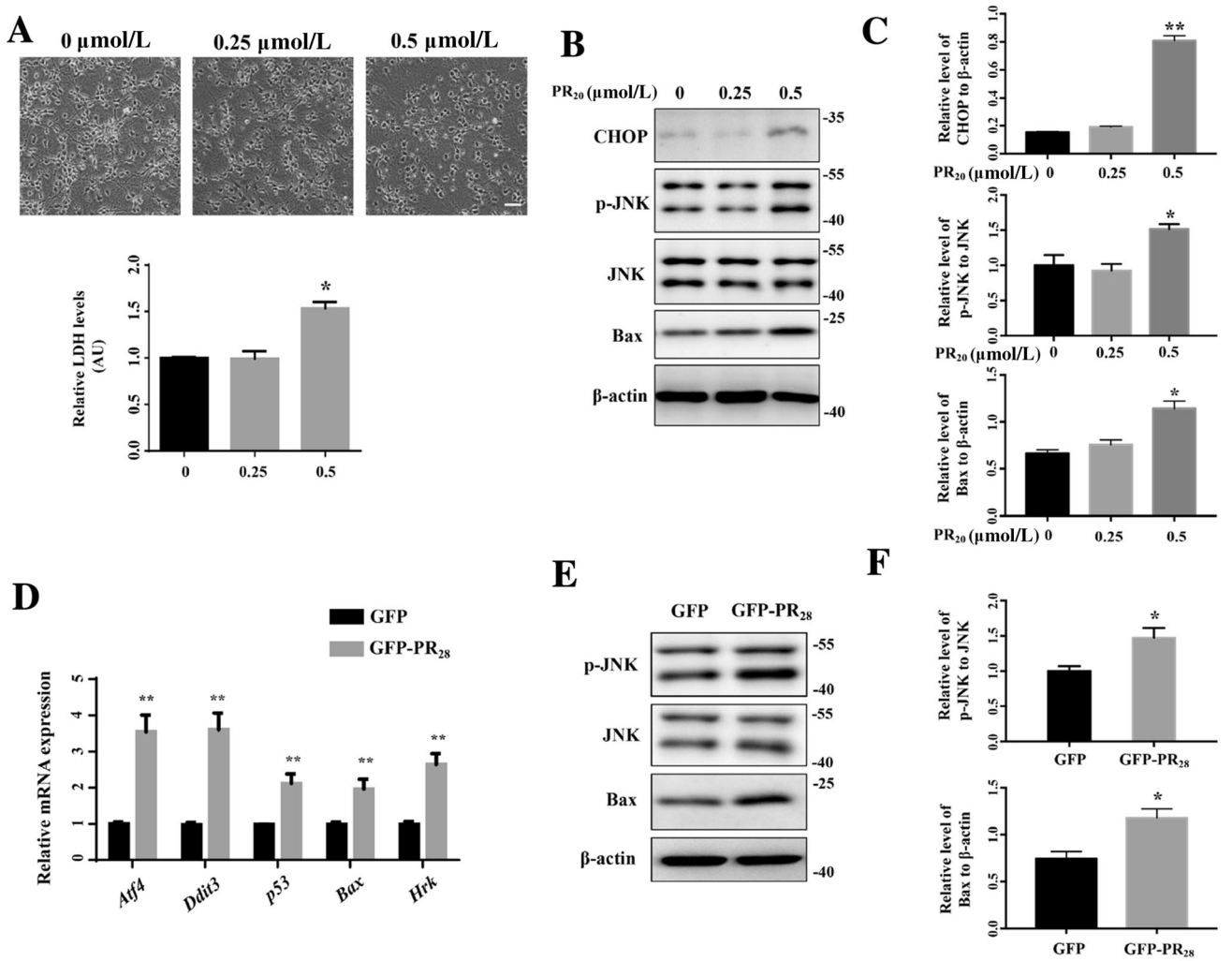

Fig. 4 Poly-PR induces the ER stress and JNK activation in primary cortical neurons of mouse**. A** Cytotoxicity measured using LDH release from primary mouse cortical neurons treated with PR_{20} (0, 0.25, or 0.5 μmol/L) for 24 h. PR_{20} resulted in cell death at 0.5 μmol/L. Values are the mean ± SEM from three independent experiments (*$P < 0.05$, one-way ANOVA and Dunnett's multiple comparisons test; scale bar, 50 μm). **B** Western blots of protein levels of CHOP, p-JNK, and Bax in primary mouse cortical neurons treated as in (A). **C** Quantitative analysis of the relative density of CHOP and Bax normalized to the loading control (β-actin), and quantitative analysis of the relative density of p-JNK normalized to the loading control (JNK). Values are the mean ± SEM from three independent experiments (*$P < 0.05$, **$P < 0.01$, one-way ANOVA and Dunnett's multiple comparisons test). **D** qRT–PCR analysis of mRNA levels of *Atf4*, *Ddit3*, *p53*, *Bax* and *Hrk* normalized to *β-actin* in primary mouse cortical neurons infected with lentivirus expressing GFP or GFP-PR_{28} for 4 days. Values are the mean ± SEM from three independent experiments (**$P < 0.01$, *t*-tests). **E** Western blots of p-JNK and Bax protein levels in primary mouse cortical neurons treated as in (D). **F** Quantitative analysis of the relative density of p-JNK normalized to the loading control (JNK), and quantitative analysis of the relative density of Bax normalized to the loading control (β-actin). Values are the mean ± SEM from three independent experiments (*$P < 0.05$, *t*-tests).

activation in primary neurons. After pretreatment with SP600125 for 12 h, the activation of phosphorylated JNK and the upregulation of p53 and Bax were suppressed in neurons treated with PR_{20} (Fig. 5A–C). Moreover, SP600125 suppressed cell death in primary neurons treated with poly-PR, as evidenced by LDH release assays (Fig. 5D). These results revealed that the expression of pro-apoptotic factors can be downregulated by inhibiting the activation of JNK, thereby preventing cell death (Fig. 5E). In order to exclude the possibility that SP600125 affects the level of PR_{20} in cells, we pretreated the cells with SP600125 for 12 h followed by treatment with synthetic PR_{20} peptides. SP600125 did not change the fluorescence intensity of FITC in these cells (Supplementary Fig. S1).

Inhibition of Clathrin-Mediated Endocytosis Suppresses the Cell Death Caused by PR_{20}

Since we had shown that chlorpromazine blocked poly-PR uptake by inhibiting clathrin-mediated endocytosis, we wondered whether chlorpromazine can suppress the cell

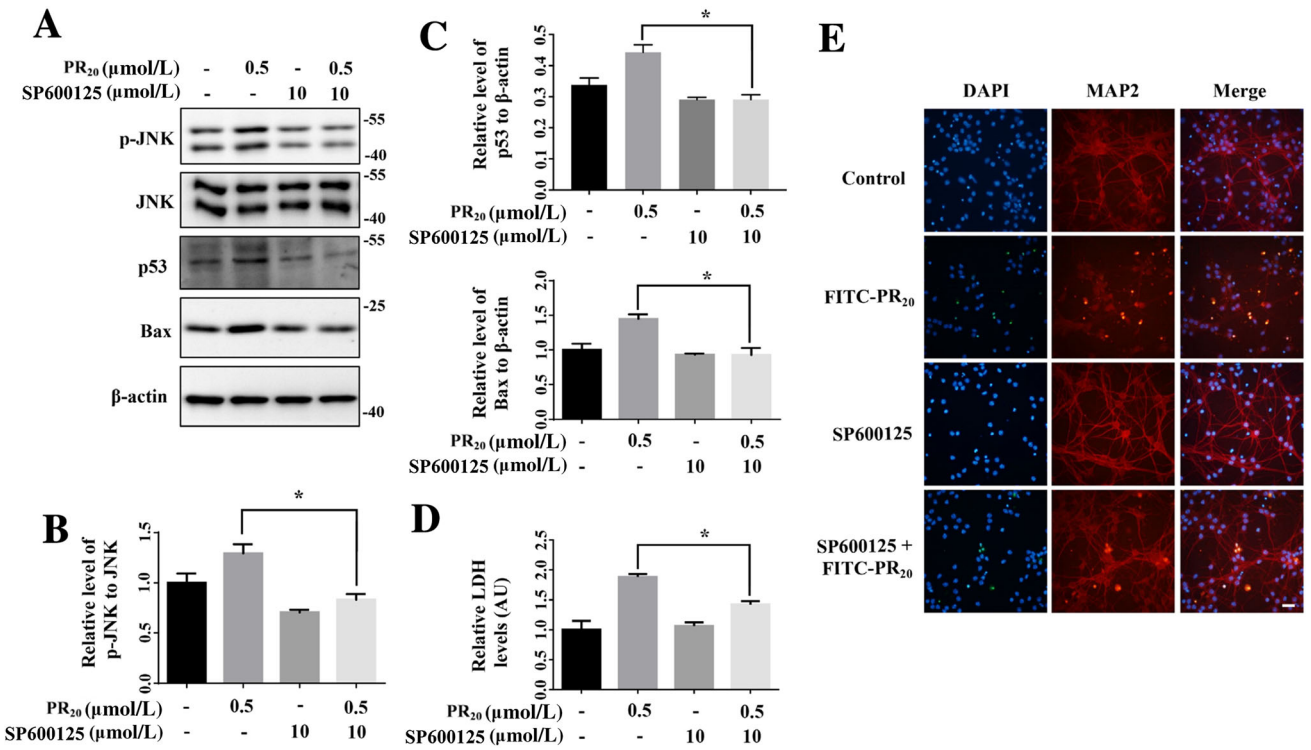

Fig. 5 JNK inhibitor SP600125 suppresses the cell death caused by PR_{20}. **A** Western blots of the protein levels of p-JNK, p53, and Bax in primary mouse cortical neurons pretreated with 10 μmol/L SP600125 for 12 h and then treated with 0.5 μmol/L PR_{20} for 24 h. **B** Quantitative analysis of the relative density of p-JNK normalized to the loading control (JNK). Values are the mean ± SEM from three independent experiments (*$P < 0.05$, two-way ANOVA and Tukey's multiple comparisons test). **C** Quantitative analysis of the relative density of p53 and Bax normalized to the loading control (β-actin). Values are the mean ± SEM from three independent experiments (*$P < 0.05$, two-way ANOVA and Tukey's multiple comparisons test). **D** Cytotoxicity measured by LDH release assay in primary mouse cortical neurons pretreated with 10 μmol/L SP600125 for 12 h and then treated with 0.5 μmol/L PR_{20} for 48 h. Values are the mean ± SEM from three independent experiments (*$P < 0.05$, two-way ANOVA and Tukey's multiple comparisons test). **E** Immunostaining for anti-MAP2 antibody in primary mouse cortical neurons treated as in (A) (blue, DAPI; green, FITC; red, MAP2; scale bar, 50 μm).

death induced by synthetic PR_{20}. We found that pretreatment with chlorpromazine markedly attenuated the poly-PR-induced cell death, as evidenced by PI staining and LDH release assays (Fig. 6A–C). The chlorpromazine pretreatment attenuated ER stress and suppressed the activation of phosphorylated JNK and the upregulation of p53 caused by poly-PR treatment (Fig. 6D, E).

Discussion

Lines of evidence indicate that the transmission of pathogenic proteins associated with neurodegenerative diseases is responsible for the induction of neurodegeneration. These disease-related proteins or peptides, such as β-amyloid, α-synuclein, SOD1, TAR DNA-binding protein 43, and poly-glutamine, have the ability to cross cellular membranes and transfer to adjacent cells, a process known as prion-like propagation [50–58]. This transfer of pathogenic proteins leads to the neuropathological spread of a lesion. Previous work has confirmed that five DPRs can spread between neurons or from neurons to glia [20]. The mechanism underlying the release and uptake of DPRs is largely unknown. In the present study, we found that the uptake of poly-PR is mediated by endocytosis. Chlorpromazine, an inhibitor of clathrin-dependent endocytosis, largely blocked poly-PR uptake, and this attenuated the cell death induced by poly-PR.

Clathrin-dependent endocytosis, which uses clathrin-coated vesicles in the cell surface, is the most common endocytic mechanism by which a cell takes up extracellular material [59]. Clathrin is a trimer of heterodimers, each unit consisting of one heavy and one light chain, making a lattice-like coat around vesicles. Adaptor proteins link a specific cargo with the clathrin-coated vesicle [38, 39]. Clathrin-dependent endocytosis is involved in the uptake of β-amyloid peptides by astrocytes [60]. Inhibition of clathrin-dependent endocytosis significantly decreases the internalization of β-amyloid peptides by astrocytes, and improves their viability [60]. Also, pathological α-synuclein can enter neurons through a clathrin-dependent

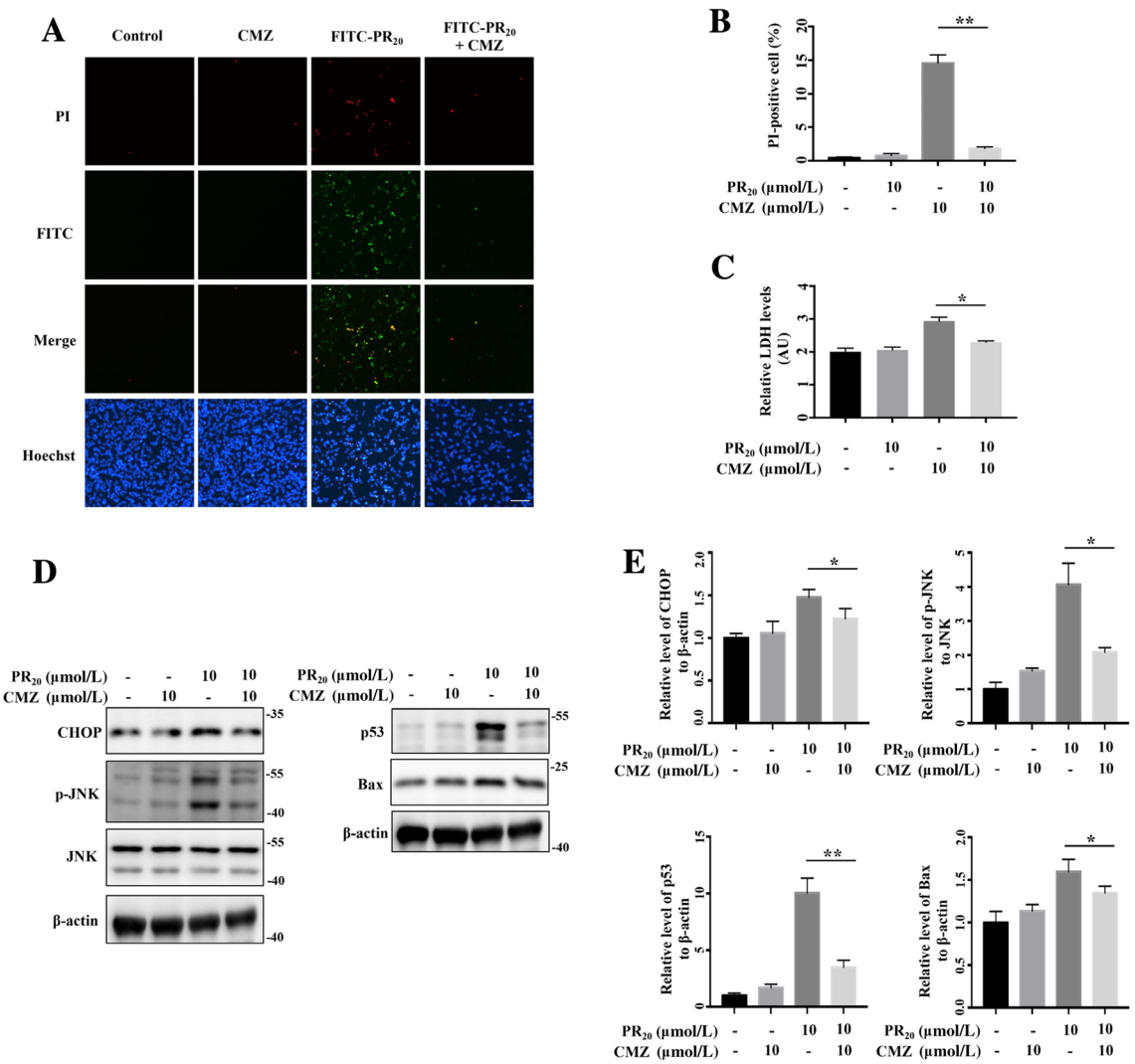

Fig. 6 Inhibition of clathrin-mediated endocytosis suppresses the cell death caused by PR_{20}. **A** PI staining to assess cell death in SH-SY5Y cells pretreated with 10 μmol/L CMZ for 30 min and then with 10 μmol/L PR_{20} for 12 h, after which the culture medium replaced with fresh medium and the cells further culture for 36 h (scale bar, 100 μm). **B** Relative integrated optical densities of PI-positive cells as in (A). Values are the mean ± SEM from three independent experiments (**$P < 0.01$, two-way ANOVA and Tukey's multiple comparisons test). **C** Cytotoxicity assessed by lactose dehydrogenase (LDH) release from SH-SY5Y cells treated as in (A). Values are the mean ± SEM from three independent experiments (*$P < 0.05$, two-way ANOVA and Tukey's multiple comparisons test). **D** Western blots of the protein levels of CHOP, p-JNK, p53, and Bax in SH-SY5Y treated as in (A). **E** Quantitative analysis of the relative density of CHOP, p53, and Bax normalized to the loading control (β-actin), and quantitative analysis of the relative density of p-JNK normalized to the loading control (JNK). Values are the mean ± SEM from three independent experiments (*$P < 0.05$, **$P < .01$, two-way ANOVA and Tukey's multiple comparisons test)

endocytic process. Blocking clathrin-dependent endocytosis inhibits the transmission of α-synuclein [61].

It has been reported that poly-GR or -PR induces cell toxicity both *in vivo* and *in vitro* [9–11, 14, 62]. Poly-GA induces ER stress though proteasome inhibition [36]. Poly-PR and poly-GR induce cell death by impairing pre-mRNA splicing and the maturation of ribosomal RNA in U2OS cells and human astrocytes [10] or by ER stress [63] and JNK activation [64].

Emerging evidence indicates that ER stress plays an important role in equilibrating protein homeostasis in cells and controlling cell fate. However, chronic ER stress damages the normal function of cells, thus initiating the apoptotic pathway [26]. Many studies have demonstrated that ER stress is associated with neurodegenerative diseases. In Alzheimer's disease, β-amyloid peptides induce ER stress in cortical neurons and cause caspase-12-dependent cell death [65]. In Parkinson's disease, α-synuclein interacts with the UPR activator glucose-regulated protein 78 (GRP78/Bip) and induces cell death by the PERK pathway [66]. α-Synuclein also inhibits the processing of ATF6 by interacting with ATF6 to activate pro-

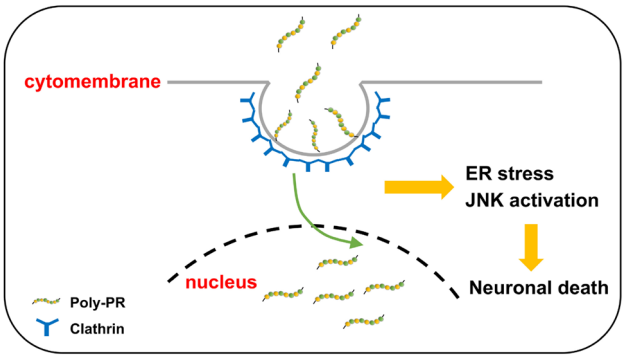

Fig. 7 Poly-PR peptides are transferred into cells by endocytosis in a clathrin-dependent manner, leading to cell death by ER stress and JNK activation.

apoptotic signaling [67]. In ALS, mutant SOD1 interacts with the ER membrane protein Derlin-1, a key regulator of ER-associated protein degradation; this induces ER stress and activates the cell death pathway that is dependent on apoptosis signal-regulating kinase 1 [68]. Recent studies have shown that ER stress contributes to neuronal death in C9-ALS [35, 36, 63]. iPSC-derived motor neurons with GGGGCC repeat expansions in *C9orf72* show activation of ER stress and dysfunction of Ca^{2+} homeostasis [36].

Chronic ER stress and JNK activation contribute to cell death by activating p53 transcription activity [69] and stimulating the transcription of Bax [70]. The JNK pathway plays an important role in signal transduction in various neurodegenerative diseases including ALS and Parkinson's disease [32, 71–73]. JNK activation is involved in several forms of motor neuronal loss induced by genetic factors [32]. Accordingly, it has been reported that JNK is activated in samples from C9-ALS patients [31]. In our experiments, poly-PR induced the phosphorylation of JNK and upregulated the expression of p53 and Bax. Inhibition of JNK by SP600125 significantly protected neurons from poly-PR-induced cell death and decreased the levels of p53 and Bax that were upregulated by poly-PR. We concluded that the JNK-mediated pathway plays an important role in poly-PR-induced neurotoxicity. As ER stress plays an important role in neurodegeneration, an inhibition of ER stress-induced JNK activation provides protective effects on neurons in our poly-PR cellular model.

Interestingly, it has been reported that Rab7 may participate in the intracellular transport of PR_{20} peptides after their endocytosis [63]. In primary cultured dorsal root ganglion neurons, knockout of Rab7 alleviates the axon degeneration induced by synthetic PR_{20} peptides and delays neuronal death [63], suggesting that a blockade of the intracellular transport of PR_{20} peptides reduces their toxicity. Most interestingly, similar effects as Rab7 knockout have been reported in *TMX2*-knockout cells [63]. That TMX2 is a response to ER stress and TMX2 deficiency reduces it [63] suggests that ER stress is involved the axon degeneration induced by PR_{20} peptides. In our experiments, PR_{20} peptide-induced ER stress and neuronal death were largely blocked by chlorpromazine, suggesting that PR_{20} peptides undergo clathrin-mediated endocytosis to enter cells and cause ER stress and toxicity.

In summary, we demonstrated that poly-PR is transferred into neurons *via* the clathrin-dependent endocytic pathway to induce ER stress and JNK activation, leading to neuronal death. Blockade of the endocytosis of PR_{20} peptides by chlorpromazine protects neurons from PR_{20} peptide toxicity (Fig.7).

Acknowledgements This work was supported by the National Natural Science Foundation of China (81761148024 and 31871023), the National Key Scientific R&D Program of China (2016YFC1306000), Suzhou Clinical Research Center of Neurological Disease (Szzx201503), and a Project Funded by the Priority Academic Program Development of Jiangsu Higher Education Institutions, China.

References

1. Taylor JP, Brown RH, Jr., Cleveland DW. Decoding ALS: from genes to mechanism. Nature 2016, 539: 197–206.
2. Wu D, Hao Z, Ren H, Wang G. Loss of VAPB Regulates Autophagy in a Beclin 1-Dependent Manner. Neurosci Bull 2018, 34: 1037–1046.
3. DeJesus-Hernandez M, Mackenzie IR, Boeve BF, Boxer AL, Baker M, Rutherford NJ, *et al.* Expanded GGGGCC hexanucleotide repeat in noncoding region of C9ORF72 causes chromosome 9p-linked FTD and ALS. Neuron 2011, 72: 245–256.
4. Renton AE, Majounie E, Waite A, Simon-Sanchez J, Rollinson S, Gibbs JR, *et al.* A hexanucleotide repeat expansion in C9ORF72 is the cause of chromosome 9p21-linked ALS-FTD. Neuron 2011, 72: 257–268.
5. Gendron TF, Bieniek KF, Zhang YJ, Jansen-West K, Ash PE, Caulfield T, *et al.* Antisense transcripts of the expanded C9ORF72 hexanucleotide repeat form nuclear RNA foci and undergo repeat-associated non-ATG translation in c9FTD/ALS. Acta Neuropathol 2013, 126: 829–844.
6. Mori K, Arzberger T, Grasser FA, Gijselinck I, May S, Rentzsch K, *et al.* Bidirectional transcripts of the expanded C9orf72 hexanucleotide repeat are translated into aggregating dipeptide repeat proteins. Acta Neuropathol 2013, 126: 881–893.
7. Zu T, Liu Y, Banez-Coronel M, Reid T, Pletnikova O, Lewis J, *et al.* RAN proteins and RNA foci from antisense transcripts in C9ORF72 ALS and frontotemporal dementia. Proc Natl Acad Sci U S A 2013, 110: E4968–4977.
8. Ash PE, Bieniek KF, Gendron TF, Caulfield T, Lin WL, Dejesus-Hernandez M, *et al.* Unconventional translation of C9ORF72 GGGGCC expansion generates insoluble polypeptides specific to c9FTD/ALS. Neuron 2013, 77: 639–646.
9. Mizielinska S, Gronke S, Niccoli T, Ridler CE, Clayton EL, Devoy A, *et al.* C9orf72 repeat expansions cause neurodegeneration in *Drosophila* through arginine-rich proteins. Science 2014, 345: 1192–1194.
10. Kwon I, Xiang S, Kato M, Wu L, Theodoropoulos P, Wang T, *et al.* Poly-dipeptides encoded by the C9orf72 repeats bind

nucleoli, impede RNA biogenesis, and kill cells. Science 2014, 345: 1139–1145.
11. Wen X, Tan W, Westergard T, Krishnamurthy K, Markandaiah SS, Shi Y, *et al.* Antisense proline-arginine RAN dipeptides linked to C9ORF72-ALS/FTD form toxic nuclear aggregates that initiate in vitro and in vivo neuronal death. Neuron 2014, 84: 1213–1225.
12. Jovicic A, Mertens J, Boeynaems S, Bogaert E, Chai N, Yamada SB, *et al.* Modifiers of C9orf72 dipeptide repeat toxicity connect nucleocytoplasmic transport defects to FTD/ALS. Nat Neurosci 2015, 18: 1226–1229.
13. Boeynaems S, Bogaert E, Michiels E, Gijselinck I, Sieben A, Jovicic A, *et al. Drosophila* screen connects nuclear transport genes to DPR pathology in c9ALS/FTD. Sci Rep 2016, 6: 20877.
14. Tao Z, Wang H, Xia Q, Li K, Li K, Jiang X, *et al.* Nucleolar stress and impaired stress granule formation contribute to C9orf72 RAN translation-induced cytotoxicity. Hum Mol Genet 2015, 24: 2426–2441.
15. Lee KH, Zhang P, Kim HJ, Mitrea DM, Sarkar M, Freibaum BD, *et al.* C9orf72 Dipeptide repeats impair the assembly, dynamics, and function of membrane-less organelles. Cell 2016, 167: 774–788 e717.
16. Lopez-Gonzalez R, Lu Y, Gendron TF, Karydas A, Tran H, Yang D, *et al.* Poly(GR) in C9ORF72-Related ALS/FTD Compromises mitochondrial function and increases oxidative stress and DNA damage in iPSC-derived motor neurons. Neuron 2016, 92: 383–391.
17. Lin Y, Mori E, Kato M, Xiang S, Wu L, Kwon I, *et al.* Toxic PR Poly-dipeptides encoded by the C9orf72 repeat expansion target LC domain polymers. Cell 2016, 167: 789–802 e712.
18. Shi KY, Mori E, Nizami ZF, Lin Y, Kato M, Xiang S, *et al.* Toxic PRn poly-dipeptides encoded by the C9orf72 repeat expansion block nuclear import and export. Proc Natl Acad Sci U S A 2017, 114: E1111–E1117.
19. Boeynaems S, Bogaert E, Kovacs D, Konijnenberg A, Timmerman E, Volkov A, *et al.* Phase separation of C9orf72 dipeptide repeats perturbs stress granule dynamics. Mol Cell 2017, 65: 1044–1055 e1045.
20. Westergard T, Jensen BK, Wen X, Cai J, Kropf E, Iacovitti L, *et al.* Cell-to-cell transmission of dipeptide repeat proteins linked to C9orf72-ALS/FTD. Cell Rep 2016, 17: 645–652.
21. Yin S, Lopez-Gonzalez R, Kunz RC, Gangopadhyay J, Borufka C, Gygi SP, *et al.* Evidence that C9ORF72 dipeptide repeat proteins associate with U2 snRNP to cause mis-splicing in ALS/FTD patients. Cell Rep 2017, 19: 2244–2256.
22. Kanekura K, Yagi T, Cammack AJ, Mahadevan J, Kuroda M, Harms MB, *et al.* Poly-dipeptides encoded by the C9ORF72 repeats block global protein translation. Hum Mol Genet 2016, 25: 1803–1813.
23. Hetz C, Saxena S. ER stress and the unfolded protein response in neurodegeneration. Nat Rev Neurol 2017, 13: 477–491.
24. Medinas DB, Valenzuela V, Hetz C. Proteostasis disturbance in amyotrophic lateral sclerosis. Hum Mol Genet 2017, 26: R91–R104.
25. Rozas P, Bargsted L, Martinez F, Hetz C, Medinas DB. The ER proteostasis network in ALS: Determining the differential motoneuron vulnerability. Neurosci Lett 2017, 636: 9–15.
26. Hetz C. The unfolded protein response: controlling cell fate decisions under ER stress and beyond. Nat Rev Mol Cell Biol 2012, 13: 89–102.
27. Walter P, Ron D. The unfolded protein response: from stress pathway to homeostatic regulation. Science 2011, 334: 1081–1086.
28. Hetz C, Mollereau B. Disturbance of endoplasmic reticulum proteostasis in neurodegenerative diseases. Nat Rev Neurosci 2014, 15: 233–249.
29. Hetz C, Chevet E, Oakes SA. Proteostasis control by the unfolded protein response. Nat Cell Biol 2015, 17: 829–838.
30. Hetz C, Papa FR. The unfolded protein response and cell fate control. Mol Cell 2018, 69: 169–181.
31. Lee S, Shang Y, Redmond SA, Urisman A, Tang AA, Li KH, *et al.* Activation of HIPK2 promotes ER stress-mediated neurodegeneration in amyotrophic lateral sclerosis. Neuron 2016, 91: 41–55.
32. Bhinge A, Namboori SC, Zhang X, VanDongen AMJ, Stanton LW. Genetic Correction of SOD1 mutant iPSCs reveals ERK and JNK activated AP1 as a Driver of neurodegeneration in amyotrophic lateral sclerosis. Stem Cell Reports 2017, 8: 856–869.
33. Kikuchi H, Almer G, Yamashita S, Guegan C, Nagai M, Xu Z, *et al.* Spinal cord endoplasmic reticulum stress associated with a microsomal accumulation of mutant superoxide dismutase-1 in an ALS model. Proc Natl Acad Sci U S A 2006, 103: 6025–6030.
34. Kiskinis E, Sandoe J, Williams LA, Boulting GL, Moccia R, Wainger BJ, *et al.* Pathways disrupted in human ALS motor neurons identified through genetic correction of mutant SOD1. Cell Stem Cell 2014, 14: 781–795.
35. Dafinca R, Scaber J, Ababneh N, Lalic T, Weir G, Christian H, *et al.* C9orf72 hexanucleotide expansions are associated with altered endoplasmic reticulum calcium homeostasis and stress granule formation in induced pluripotent stem cell-derived neurons from patients with amyotrophic lateral sclerosis and frontotemporal dementia. Stem Cells 2016, 34: 2063–2078.
36. Zhang YJ, Jansen-West K, Xu YF, Gendron TF, Bieniek KF, Lin WL, *et al.* Aggregation-prone c9FTD/ALS poly(GA) RAN-translated proteins cause neurotoxicity by inducing ER stress. Acta Neuropathol 2014, 128: 505–524.
37. Grant BD, Donaldson JG. Pathways and mechanisms of endocytic recycling. Nat Rev Mol Cell Biol 2009, 10: 597–608.
38. Kumari S, Mg S, Mayor S. Endocytosis unplugged: multiple ways to enter the cell. Cell Res 2010, 20: 256–275.
39. McMahon HT, Boucrot E. Molecular mechanism and physiological functions of clathrin-mediated endocytosis. Nat Rev Mol Cell Biol 2011, 12: 517–533.
40. Xia Q, Hu Q, Wang H, Yang H, Gao F, Ren H, *et al.* Induction of COX-2-PGE2 synthesis by activation of the MAPK/ERK pathway contributes to neuronal death triggered by TDP-43-depleted microglia. Cell Death Dis 2015, 6: e1702.
41. Chen D, Li YP, Yu YX, Zhou T, Liu C, Fei EK, *et al.* Dendritic cell nuclear protein-1 regulates melatonin biosynthesis by binding to BMAL1 and inhibiting the transcription of N-acetyltransferase in C6 cells. Acta Pharmacol Sin 2018, 39: 597–606.
42. Fu K, Wang Y, Guo D, Wang G, Ren H. Familial Parkinson's disease-associated L166P mutant DJ-1 is cleaved by mitochondrial serine protease Omi/HtrA2. Neurosci Bull 2017, 33: 685–694.
43. Guo DK, Zhu Y, Sun HY, Xu XY, Zhang S, Hao ZB, *et al.* Pharmacological activation of REV-ERBalpha represses LPS-induced microglial activation through the NF-kappaB pathway. Acta Pharmacol Sin 2018.
44. Yumoto R, Nishikawa H, Okamoto M, Katayama H, Nagai J, Takano M. Clathrin-mediated endocytosis of FITC-albumin in alveolar type II epithelial cell line RLE-6TN. Am J Physiol Lung Cell Mol Physiol 2006, 290: L946–955.
45. Wang LH, Rothberg KG, Anderson RG. Mis-assembly of clathrin lattices on endosomes reveals a regulatory switch for coated pit formation. J Cell Biol 1993, 123: 1107–1117.
46. Nabi IR, Le PU. Caveolae/raft-dependent endocytosis. J Cell Biol 2003, 161: 673–677.
47. Ikehata M, Yumoto R, Nakamura K, Nagai J, Takano M. Comparison of albumin uptake in rat alveolar type II and type

I-like epithelial cells in primary culture. Pharm Res 2008, 25: 913–922.
48. Nakase I, Niwa M, Takeuchi T, Sonomura K, Kawabata N, Koike Y, *et al.* Cellular uptake of arginine-rich peptides: roles for macropinocytosis and actin rearrangement. Mol Ther 2004, 10: 1011–1022.
49. Sovolyova N, Healy S, Samali A, Logue SE. Stressed to death - mechanisms of ER stress-induced cell death. Biol Chem 2014, 395: 1–13.
50. Harris JA, Devidze N, Verret L, Ho K, Halabisky B, Thwin MT, *et al.* Transsynaptic progression of amyloid-beta-induced neuronal dysfunction within the entorhinal-hippocampal network. Neuron 2010, 68: 428–441.
51. Nath S, Agholme L, Kurudenkandy FR, Granseth B, Marcusson J, Hallbeck M. Spreading of neurodegenerative pathology via neuron-to-neuron transmission of beta-amyloid. J Neurosci 2012, 32: 8767–8777.
52. Meyer-Luehmann M, Coomaraswamy J, Bolmont T, Kaeser S, Schaefer C, Kilger E, *et al.* Exogenous induction of cerebral beta-amyloidogenesis is governed by agent and host. Science 2006, 313: 1781–1784.
53. Desplats P, Lee HJ, Bae EJ, Patrick C, Rockenstein E, Crews L, *et al.* Inclusion formation and neuronal cell death through neuron-to-neuron transmission of alpha-synuclein. Proc Natl Acad Sci U S A 2009, 106: 13010–13015.
54. Kanouchi T, Ohkubo T, Yokota T. Can regional spreading of amyotrophic lateral sclerosis motor symptoms be explained by prion-like propagation? J Neurol Neurosurg Psychiatry 2012, 83: 739–745.
55. Feiler MS, Strobel B, Freischmidt A, Helferich AM, Kappel J, Brewer BM, *et al.* TDP-43 is intercellularly transmitted across axon terminals. J Cell Biol 2015, 211: 897–911.
56. Ren PH, Lauckner JE, Kachirskaia I, Heuser JE, Melki R, Kopito RR. Cytoplasmic penetration and persistent infection of mammalian cells by polyglutamine aggregates. Nat Cell Biol 2009, 11: 219–225.
57. Silverman JM, Fernando SM, Grad LI, Hill AF, Turner BJ, Yerbury JJ, *et al.* Disease mechanisms in ALS: Misfolded SOD1 transferred through exosome-dependent and exosome-independent pathways. Cell Mol Neurobiol 2016, 36: 377–381.
58. Wu X, Zheng T, Zhang B. Exosomes in Parkinson's disease. Neurosci Bull 2017, 33: 331–338.
59. Mousavi SA, Malerod L, Berg T, Kjeken R. Clathrin-dependent endocytosis. Biochem J 2004, 377: 1–16.
60. Dominguez-Prieto M, Velasco A, Tabernero A, Medina JM. Endocytosis and transcytosis of amyloid-beta peptides by astrocytes: a possible mechanism for amyloid-beta clearance in Alzheimer's disease. J Alzheimers Dis 2018, 65: 1109–1124.
61. Oh SH, Kim HN, Park HJ, Shin JY, Bae EJ, Sunwoo MK, *et al.* Mesenchymal stem cells inhibit transmission of alpha-synuclein by modulating clathrin-mediated endocytosis in a Parkinsonian model. Cell Rep 2016, 14: 835–849.
62. Zhang YJ, Gendron TF, Ebbert MTW, O'Raw AD, Yue M, Jansen-West K, *et al.* Poly(GR) impairs protein translation and stress granule dynamics in C9orf72-associated frontotemporal dementia and amyotrophic lateral sclerosis. Nat Med 2018, 24: 1136–1142.
63. Kramer NJ, Haney MS, Morgens DW, Jovicic A, Couthouis J, Li A, *et al.* CRISPR-Cas9 screens in human cells and primary neurons identify modifiers of C9ORF72 dipeptide-repeat-protein toxicity. Nat Genet 2018, 50: 603–612.
64. Suzuki H, Shibagaki Y, Hattori S, Matsuoka M. The proline-arginine repeat protein linked to C9-ALS/FTD causes neuronal toxicity by inhibiting the DEAD-box RNA helicase-mediated ribosome biogenesis. Cell Death Dis 2018, 9: 975.
65. Nakagawa T, Zhu H, Morishima N, Li E, Xu J, Yankner BA, *et al.* Caspase-12 mediates endoplasmic-reticulum-specific apoptosis and cytotoxicity by amyloid-beta. Nature 2000, 403: 98–103.
66. Bellucci A, Navarria L, Zaltieri M, Falarti E, Bodei S, Sigala S, *et al.* Induction of the unfolded protein response by alpha-synuclein in experimental models of Parkinson's disease. J Neurochem 2011, 116: 588–605.
67. Credle JJ, Forcelli PA, Delannoy M, Oaks AW, Permaul E, Berry DL, *et al.* alpha-Synuclein-mediated inhibition of ATF6 processing into COPII vesicles disrupts UPR signaling in Parkinson's disease. Neurobiol Dis 2015, 76: 112–125.
68. Nishitoh H, Kadowaki H, Nagai A, Maruyama T, Yokota T, Fukutomi H, *et al.* ALS-linked mutant SOD1 induces ER stress- and ASK1-dependent motor neuron death by targeting Derlin-1. Genes Dev 2008, 22: 1451–1464.
69. Buschmann T, Yin Z, Bhoumik A, Ronai Z. Amino-terminal-derived JNK fragment alters expression and activity of c-Jun, ATF2, and p53 and increases H2O2-induced cell death. J Biol Chem 2000, 275: 16590–16596.
70. Mandal M, Olson DJ, Sharma T, Vadlamudi RK, Kumar R. Butyric acid induces apoptosis by up-regulating Bax expression via stimulation of the c-Jun N-terminal kinase/activation protein-1 pathway in human colon cancer cells. Gastroenterology 2001, 120: 71–78.
71. Wang W, Wen D, Duan W, Yin J, Cui C, Wang Y, *et al.* Systemic administration of scAAV9-IGF1 extends survival in SOD1(G93A) ALS mice via inhibiting p38 MAPK and the JNK-mediated apoptosis pathway. Brain Res Bull 2018, 139: 203–210.
72. He H, Wang S, Tian J, Chen L, Zhang W, Zhao J, *et al.* Protective effects of 2,3,5,4'-tetrahydroxystilbene-2-O-beta-D-glucoside in the MPTP-induced mouse model of Parkinson's disease: Involvement of reactive oxygen species-mediated JNK, P38 and mitochondrial pathways. Eur J Pharmacol 2015, 767: 175–182.
73. Peng J, Andersen JK. The role of c-Jun N-terminal kinase (JNK) in Parkinson's disease. IUBMB Life 2003, 55: 267–271.